Finite-time sliding mode synchronization of chaotic systems*

Ni Jun-Kang(倪骏康)†, Liu Chong-Xin(刘崇新), Liu Kai(刘 凯), and Liu Ling(刘 凌)‡

[a] State Key Laboratory of Electrical Insulation and Power Equipment, Xi'an Jiaotong University, Xi'an 710049, China
[b] School of Electrical Engineering, Xi'an Jiaotong University, Xi'an 710049, China

(Received 23 February 2014; revised manuscript received 6 April 2014; published online 20 August 2014)

A new finite-time sliding mode control approach is presented for synchronizing two different topological structure chaotic systems. With the help of the Lyapunov method, the convergence property of the proposed control strategy is discussed in a rigorous manner. Furthermore, it is mathematically proved that our control strategy has a faster convergence speed than the conventional finite-time sliding mode control scheme. In addition, the proposed control strategy can ensure the finite-time synchronization between the master and the slave chaotic systems under internal uncertainties and external disturbances. Simulation results are provided to show the speediness and robustness of the proposed scheme. It is worth noticing that the proposed control scheme is applicable for secure communications.

Keywords: finite-time control, sliding mode control, chaos synchronization, secure communication

PACS: 05.45.Gg, 05.45.Xt, 05.45.Pq **DOI:** 10.1088/1674-1056/23/10/100504

1. Introduction

In recent years, chaos synchronization, one of the hot topics in nonlinear science, has attracted much attention from scientists from the fields of mathematics, physics and engineering due to its wide and powerful applications in secure communication,[1] network synchronization,[2] ecological systems,[3] the human system,[4] telecommunications,[5] laser dynamics,[6] power converters,[7] permanent magnet synchronous motors,[8] information processing,[9] and many other fields.[10] Since Pecora and Carroll[11] proved that chaotic systems could be synchronized and realized a synchronization between chaotic circuits, a wide variety of control strategies have been proposed to synchronize different chaotic systems, such as active control,[12] backstepping control,[13] impulsive control,[14] intermittent control,[15] adaptive control,[16] H_∞ control,[17] projective synchronization,[18] linear matrix inequality techniques,[19] feedback control,[20] fuzzy logic control,[21] state observer control,[22] and passive control.[23]

However, in many control schemes, the convergence time cannot be assigned in advance. In other words, the slave system cannot synchronize with the master system within a prespecified convergence time. From a practical point of view, it is more advisable to realize synchronization within a prespecified convergence time. Taking the secure communication for example, if the designers know the convergence time, they can know when the encrypted information can be recovered completely; moreover, if the synchronization can be achieved within a shorter time, more valuable information can be recovered. The finite-time control can achieve synchronization within a given finite time and minimize the convergence time. These advantages attract many scientists to study the applications of the finite-time control in chaos synchronization. Chuang *et al.*[24] used a simple linear control to achieve synchronization between generalized Lorenz systems within a finite time. Cai *et al.*[25] proposed a finite-time control scheme to realize synchronization between chaotic systems with different orders. Liu[26] designed a robust finite-time controller to stabilize unified chaotic systems with certain and uncertain parameters. Gholizadeh *et al.*[27] reported an optimized finite-time control to stabilize the chaotic oscillation in a power system and proved that the proposed controller has a faster convergence rate than a nonlinear conventional controller. Aghababa and Feizi[28] investigated finite-time synchronization between chaotic systems with model uncertainty and external disturbance. Vincent and Guo[29] used an adaptive feedback control to achieve the finite-time synchronization for a class of chaotic and hyperchaotic systems.

Combining the finite-time control with the sliding mode control can take the advantages of the finite-time control in minimizing the synchronization time and the advantages of the sliding mode control in robustness and disturbance rejection. Therefore, the finite-time sliding mode control has attracted many scientists' attention. Wang *et al.*[30] used only one finite-time terminal sliding mode control input to get rid of unmatched uncertainties and the input nonlinearity in Liu chaotic system. Wang *et al.*[31] designed a new fractional terminal sliding mode controller to ensure the occurrence of sliding motion within a finite time. A nonsingular terminal

*Project supported by the National Natural Science Foundation of China (Grant Nos. 51177117 and 51307130) and the Creative Research Groups Fund of the National Natural Science Foundation of China (Grant No. 51221005).

†Corresponding author. E-mail: max12391@126.com
‡Corresponding author. E-mail: liul@mail.xjtu.edu.cn

© 2014 Chinese Physical Society and IOP Publishing Ltd

sliding mode control[32] has been proposed to tackle the singularity in the finite-time terminal sliding mode control, and the adaptive finite-time sliding mode control[33] has been used to suppress uncertain parameters and unknown disturbances in chaotic systems. Liu *et al.*[34] introduced a fuzzy basis function network to estimate the bound of the parameter uncertainty as well as the disturbance, and used a global sliding mode controller to realize synchrony.

In this paper, we propose a new finite-time sliding mode control scheme to synchronize two different chaotic systems. Compared with the conventional finite-time sliding mode control, which has the form $\dot{s} = -k|s|^{\alpha}\,\mathrm{sign}(s)$ as reported in Refs. [28] and [35]–[38], our proposed control scheme has a fast convergence rate as shown by theoretical derivation and numerical simulation. The simulation results show the speediness and the robustness of the proposed control strategy. Finally, we apply our control scheme to secure communications and achieve satisfactory results.

The rest of this paper is organized as follows. The problem formulation and preliminaries are given in Section 2. In Section 3, the finite-time sliding mode controller is designed for synchronizing two chaotic systems. The simulation results are presented to demonstrate the effectiveness of the approach in Section 4. Section 5 contains the conclusion.

2. Problem formulation and preliminaries

Proposition 1 For any variable x with initial value $x_0 > 0$, if the dynamics of x satisfies

$$\dot{x} = -k_1 x - k_2 \mathrm{sign}(x), \quad k_1, k_2 > 0, \tag{1}$$

or

$$\dot{x} = -k_3 |x|^{\alpha} \mathrm{sign}(x), \quad k_3 > 0, 0 < \alpha < 1, \tag{2}$$

it will converge to the origin within a finite time.

Proof Defining a positive definite Lyapunov function as $V = \frac{1}{2}x^2$ and taking the time derivative of V along the trajectories of Eq. (1), we have

$$\dot{V} = x\dot{x} = -k_1 x^2 - k_2 |x| \le 0. \tag{3}$$

Similarly, the derivative of V with respect to time along the trajectories of Eq. (2) is

$$\begin{aligned} \dot{V} &= x\dot{x} = -k_3 |x|^{\alpha+1} = -k_3 (2V)^{(\alpha+1)/2} \\ &= -cV^{(\alpha+1)/2} \le 0, \end{aligned} \tag{4}$$

where $c = k_3 2^{(\alpha+1)/2}$. Thus, the trajectories of x in Eqs. (1) and (2) will converge to the origin within the finite time determined respectively by the following equations:

$$T_1 = \frac{1}{k_1} \ln\left(\frac{k_1 x_0 + k_2}{k_2}\right), \tag{5}$$

$$T_2 = \frac{|x_0|^{1-\alpha}}{k_3(1-\alpha)}. \tag{6}$$

Proposition 2 For variable x with initial value $x_0 < \mathrm{e}$, if $k_2 = k_3$ holds, the convergence time of x in Eq. (1) is shorter than that in Eq. (2)

Proof From Eq. (5), we can obtain the following inequality:

$$T_1 = \frac{1}{k_1} \ln\left(1 + \frac{k_1 x_0}{k_2}\right) < \frac{1}{k_1} \frac{k_1 x_0}{k_2} = \frac{x_0}{k_2}. \tag{7}$$

Let $T_0 = x_0/k_2$ and $f(\beta) = x_0^{\beta}/\beta$, then T_0 and T_2 can be expressed as

$$T_0 = \frac{f(1)}{k_2}, \quad T_2 = \frac{f(1-\alpha)}{k_3}. \tag{8}$$

The differentiation of $f(\beta)$ is

$$\frac{\mathrm{d}f}{\mathrm{d}\beta} = \frac{x_0^{\beta}(\beta \ln x_0 - 1)}{\beta^2}. \tag{9}$$

When the initial condition satisfies $x_0 < \mathrm{e}$, for any β that satisfies $0 < \beta < 1$, the inequality $\mathrm{d}f/\mathrm{d}\beta < 0$ holds.

When $k_2 = k_3$, the relationship between T_0, T_1, and T_2 can be obtained as $T_0 < T_2$ and $T_1 < T_2$.

Remark 1 Equation (4) is a common form of the finite-time control; however, we prove that it does not take the least time to reach the origin.

3. Synchronization of chaotic systems via a finite-time sliding mode controller

3.1. Chaos synchronization under no disturbances or uncertainties

Our goal is to design a finite-time sliding mode controller for synchronizing different chaotic systems under no disturbances or uncertainties.

Consider two chaotic systems

$$\begin{cases} \dot{x}_1 = A_1 \boldsymbol{x} + f_1(\boldsymbol{x}), \\ \dot{x}_2 = A_2 \boldsymbol{x} + f_2(\boldsymbol{x}), \\ \dot{x}_3 = A_3 \boldsymbol{x} + f_3(\boldsymbol{x}), \end{cases} \tag{10}$$

$$\begin{cases} \dot{y}_1 = B_1 \boldsymbol{y} + g_1(\boldsymbol{y}) + u_1, \\ \dot{y}_2 = B_2 \boldsymbol{y} + g_2(\boldsymbol{y}) + u_2, \\ \dot{y}_3 = B_3 \boldsymbol{y} + g_3(\boldsymbol{y}) + u_3, \end{cases} \tag{11}$$

which are the master system and the slave system respectively. Here $x_i \in \boldsymbol{x}$ and $y_i \in \boldsymbol{y}$ $(i = 1,2,3)$ denote the system states, and $f_i(\boldsymbol{x})$ and $g_i(\boldsymbol{y})$ $(i = 1,2,3)$ are continuous nonlinear smooth functions that satisfy the Lipschitz conditions:

$$|f_i(x_1) - f_i(x_2)| \le L_1 |x_1 - x_2| \forall x_1, x_2 \in \mathbf{R} \text{ for } L_1 > 0, \tag{12}$$

$$|g_i(y_1) - g_i(y_2)| \le L_2 |y_1 - y_2| \forall y_1, y_2 \in \mathbf{R} \text{ for } L_2 > 0. \tag{13}$$

Define the error between the master system and the slave system as $\boldsymbol{e} = \boldsymbol{y} - \boldsymbol{x}$, then the error system can be described as

$$\begin{cases} \dot{e}_1 = B_1 \boldsymbol{y} - A_1 \boldsymbol{x} + g_1(\boldsymbol{y}) - f_1(\boldsymbol{x}) + u_1, \\ \dot{e}_2 = B_2 \boldsymbol{y} - A_2 \boldsymbol{x} + g_2(\boldsymbol{y}) - f_2(\boldsymbol{x}) + u_2, \\ \dot{e}_3 = B_3 \boldsymbol{y} - A_3 \boldsymbol{x} + g_3(\boldsymbol{y}) - f_3(\boldsymbol{x}) + u_3. \end{cases} \tag{14}$$

To stabilize the error system within a finite time, the sliding surface can be constructed as

$$s_i(t) = e_i(t) + k_1 \int_0^t \text{sign}(e_i(\tau))\,\mathrm{d}\tau + k_2 \int_0^t e_i(\tau)\,\mathrm{d}\tau. \quad (15)$$

Theorem 1 System (14) will converge to zero within a finite time in the sliding motion.

Proof When system (14) is in the sliding motion, its motion is confined to the sliding surface

$$S(t) = \{e | s(e) = 0\}, \quad (16)$$

and satisfies the following condition:

$$\dot{s}(e) = 0, \quad (17)$$

that is,

$$\dot{e}_i = -k_2 e_i - k_1 \text{sign}(e_i), \quad (18)$$

which can guarantee that the state trajectory e_i stays on the sliding manifold $S(t)$ continuously. According to Proposition 1, the error system state variable $e_i(t)$ will converge to zero within a finite time.

Theorem 2 Let the sliding surface be Eq. (15) and the control input be

$$\begin{aligned} u_i \;=\; & A_i\boldsymbol{x} - B_i\boldsymbol{y} + f_i(\boldsymbol{x}) - g_i(\boldsymbol{y}) \\ & - k_1 \text{sign}(e_i) - k_2 e_i - k_3 \text{sign}(s_i) - k_4 s_i, \end{aligned} \quad (19)$$

then the state of error system (14) will reach the sliding surface within a finite time.

Proof Taking the time derivative of $s_i(t)$ yields

$$\dot{s}_i = \dot{e}_i + k_1 \text{sign}(e_i) + k_2 e_i = -k_4 s_i - k_3 \text{sign}(s_i). \quad (20)$$

On the basis of Proposition 1, the error system state will reach the sliding surface $s_i(t)$ within a finite time.

3.2. Chaos synchronization under uncertainties and disturbances

Adding internal uncertainties $\Delta f_i(x)$, $\Delta g_i(y)$ and external disturbances d_i^{s}, d_i^{m} to each term of the master system and the slave system yields

$$\begin{cases} \dot{x}_1 = A_1\boldsymbol{x} + f_1(\boldsymbol{x}) + \Delta f_1(\boldsymbol{x}) + d_1^{\text{m}}, \\ \dot{x}_2 = A_2\boldsymbol{x} + f_2(\boldsymbol{x}) + \Delta f_2(\boldsymbol{x}) + d_2^{\text{m}}, \\ \dot{x}_3 = A_3\boldsymbol{x} + f_3(\boldsymbol{x}) + \Delta f_3(\boldsymbol{x}) + d_3^{\text{m}}, \end{cases} \quad (21)$$

$$\begin{cases} \dot{y}_1 = B_1\boldsymbol{y} + g_1(\boldsymbol{y}) + \Delta g_1(\boldsymbol{y}) + d_1^{\text{s}} + u_1, \\ \dot{y}_2 = B_2\boldsymbol{y} + g_2(\boldsymbol{y}) + \Delta g_2(\boldsymbol{y}) + d_2^{\text{s}} + u_2, \\ \dot{y}_3 = B_3\boldsymbol{y} + g_3(\boldsymbol{y}) + \Delta g_3(\boldsymbol{y}) + d_3^{\text{s}} + u_3. \end{cases} \quad (22)$$

Assumption 1 We assume that positive constants α_i and β_i exist such that the internal uncertainties are bounded as follows:

$$|\Delta f_i(\boldsymbol{x})| \le \alpha_i |x_i|, \quad |\Delta g_i(\boldsymbol{y})| \le \beta_i |y_i|. \quad (23)$$

Assumption 2 We assume that the external disturbances are bounded as follows:

$$|d_i^{\text{s}}| \le D_i^{\text{s}}, \quad |d_i^{\text{m}}| \le D_i^{\text{m}}. \quad (24)$$

The dynamics of the error system can be obtained by subtracting Eq. (21) from Eq. (22)

$$\begin{cases} \dot{e}_1 = B_1\boldsymbol{y} - A_1\boldsymbol{x} + g_1(\boldsymbol{y}) - f_1(\boldsymbol{x}) + \Delta g_1(\boldsymbol{y}) \\ \qquad - \Delta f_1(\boldsymbol{x}) + d_1^{\text{s}} - d_1^{\text{m}} + u_1, \\ \dot{e}_2 = B_2\boldsymbol{y} - A_2\boldsymbol{x} + g_2(\boldsymbol{y}) - f_2(\boldsymbol{x}) + \Delta g_2(\boldsymbol{y}) \\ \qquad - \Delta f_2(\boldsymbol{x}) + d_2^{\text{s}} - d_2^{\text{m}} + u_2, \\ \dot{e}_3 = B_3\boldsymbol{y} - A_3\boldsymbol{x} + g_3(\boldsymbol{y}) - f_3(\boldsymbol{x}) + \Delta g_3(\boldsymbol{y}) \\ \qquad - \Delta f_3(\boldsymbol{x}) + d_3^{\text{s}} - d_3^{\text{m}} + u_3. \end{cases} \quad (25)$$

To synchronize the systems within a finite time, we select Eq. (15) as the sliding surface.

When system (25) is in the sliding motion, its motion satisfies the following condition:

$$\dot{e}_i = -k_2 e_i - k_1 \text{sign}(e_i), \quad (26)$$

which can guarantee that the state trajectory e_i stays on the sliding manifold $S(t)$continuously. Consequently, by utilizing Proposition 1, we can conclude that the error system state variable $e_i(t)$ will be stabilized to zero within a finite time.

Accordingly, the control input can be formulated as

$$\begin{aligned} u_i \;=\; & A_i\boldsymbol{x} - B_i\boldsymbol{y} + f_i(\boldsymbol{x}) - g_i(\boldsymbol{y}) \\ & - (\alpha_i |x_i| + \beta_i |y_i| + D_i^{\text{s}} + D_i^{\text{m}}) \text{sign}(s_i) \\ & - k_1 \text{sign}(e_i) - k_2 e_i - k_3 \text{sign}(s_i) - k_4 s_i. \end{aligned} \quad (27)$$

Consider candidate Lyapunov function $V = \frac{1}{2} s_i^2$. The derivative of V along the trajectory of system (25) can be calculated as

$$\begin{aligned} \dot{V} \;=\; & s_i \dot{s}_i = s_i(\dot{e}_i + k_1 \text{sign}(e_i) + k_2 e_i) \\ =\; & s_i(\Delta g_i(\boldsymbol{y}) - \Delta f_i(x) + d_i^{\text{s}} - d_i^{\text{m}} \\ & - (\alpha_i |x_i| + \beta_i |y_i| + D_i^{\text{s}} + D_i^{\text{m}}) \text{sign}(s_i) \\ & - k_3 \text{sign}(s_i) - k_4 s_i) \\ =\; & s_i(\Delta g_i(y) - \Delta f_i(x) + d_i^{\text{s}} - d_i^{\text{m}}) \\ & - |s_i| (\alpha_i |x_i| + \beta_i |y_i| + D_i^{\text{s}} + D_i^{\text{m}}) \\ & - (k_3 |s_i| + k_4 s_i^2) \le -(k_3 |s_i| + k_4 s_i^2) \le 0, \end{aligned} \quad (28)$$

which has the same form as that of Eq. (3). Therefore, we prove that the state of system (25) will reach the sliding surface and converge to the origin within a finite time.

Remark 2 Since the control law contains a discontinuous sign function, it may induce a chattering phenomenon. In order to avoid chattering, we replace sign function $\text{sign}(x)$ by continuous function $x/(|x| + \varepsilon)$, where ε is a sufficiently small positive constant.[39] In the following simulations, we choose $\varepsilon = 0.001$.

4. Numerical simulations

In this section, three illustrative examples are given to validate the speediness, robustness and feasibility of the proposed finite-time sliding mode control scheme in synchronizing two different chaotic systems. The simulations are performed using Matlab/simulink and ode45 solver that employs variable step fourth and fifth order Runge–Kutta method.

4.1. Example 1: Synchronize chaotic systems with no disturbances or uncertainties

In Ref. [40], Liu developed a new three-dimensional autonomous chaotic system containing a quadratic term, which evolved from Liu chaotic system.[41] In this example, we assume the new chaotic system to be the master system and a Lorenz system[42] to be the slave system.

The master system is given by

$$\begin{cases} \dot{x}_1 = 0.5(-x_1) + x_2^2, \\ \dot{x}_2 = 2.5x_2 - x_1x_3, \\ \dot{x}_3 = x_2 - 4x_3. \end{cases} \tag{29}$$

The slave system is given by

$$\begin{cases} \dot{y}_1 = 10(y_2 - y_1), \\ \dot{y}_2 = 30y_1 - y_2 - y_1y_3, \\ \dot{y}_3 = -\dfrac{8}{3}y_3 + y_1y_2. \end{cases} \tag{30}$$

The initial values of the new chaotic system are selected as $(x_1(0), x_2(0), x_3(0)) = (1.4, 1.6, 1.3)$, and the initial states of the Lorenz system are chosen as $(y_1(0), y_2(0), y_3(0)) = (1.8, 1.9, 1.5)$. The phase portraits of the two chaotic systems are depicted in Figs. 1 and 2, respectively.

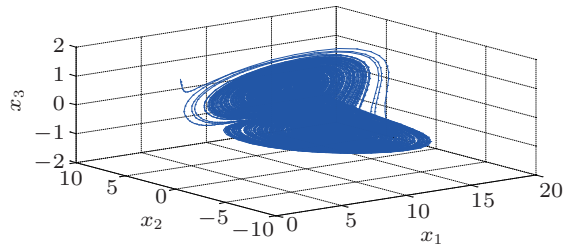


Fig. 1. (color online) Phase portraits of the new chaotic system.

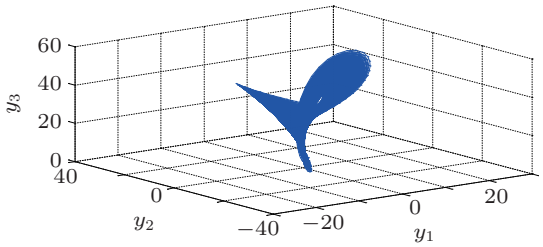


Fig. 2. (color online) Phase portraits of the Lorenz chaotic system.

Subsequently, the sliding surface of the proposed finite-time sliding mode control can be chosen as

$$s_i(t) = e_i(t) + 5\int_0^t \frac{e_i(\tau)}{|e_i(\tau)| + \varepsilon}\,\mathrm{d}\tau + 10\int_0^t e_i(\tau)\,\mathrm{d}\tau, \quad (i = 1,2,3), \tag{31}$$

and the control law can be derived as follows:

$$u_i = A_i\boldsymbol{x} - B_i\boldsymbol{y} + f_i(\boldsymbol{x}) - g_i(\boldsymbol{y}) - 5\frac{e_i}{|e_i| + \varepsilon} - 10e_i - 5\frac{s_i}{|s_i| + \varepsilon} - 10s_i, \quad (i = 1,2,3). \tag{32}$$

The evolution of the synchronization errors of the proposed finite-time sliding mode control strategy is illustrated in Fig. 3. It can be observed that the synchronization errors converge to zero rapidly, indicating that the trajectories of the slave system rapidly track the trajectories of the master system.

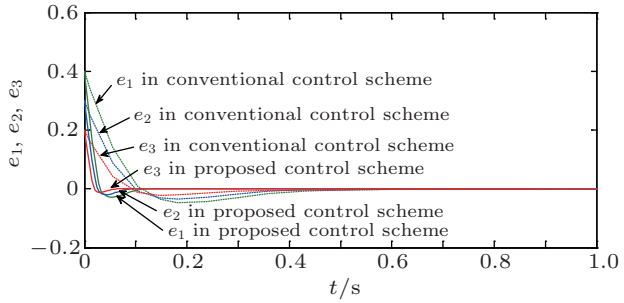


Fig. 3. (color online) Evolutions of the synchronization errors between the new system and the Lorenz system in the conventional control scheme (dashed lines) and the proposed control scheme (solid lines).

In order to show the advantage of the proposed control scheme in the convergence rate, we compare our approach with the conventional finite-time sliding mode synchronization.

The sliding surface of the conventional finite-time sliding mode control can be designed as

$$s_i(t) = e_i(t) + \sigma\int_0^t |e_i(\tau)|^\mu \frac{e_i(\tau)}{|e_i(\tau)| + \varepsilon}\,\mathrm{d}\tau, \quad (i = 1,2,3), \quad 0 < \mu < 1, \tag{33}$$

and the control law can be defined as

$$u_i = A_i\boldsymbol{x} - B_i\boldsymbol{y} + f_i(\boldsymbol{x}) - g_i(\boldsymbol{y}) - \sigma|e_i|^\mu \frac{e_i}{|e_i| + \varepsilon} - \sigma|s_i|^\mu \frac{s_i}{|s_i| + \varepsilon}, \quad (i = 1,2,3). \tag{34}$$

The parameter can be selected as $\sigma = 5$ and $\mu = 0.6$.

Remark 3 When the trajectories are on the sliding surface, the dynamic evolution of the error system states satisfies

$$\dot{e}_i \approx -\sigma|e_i|^\mu \operatorname{sign}(e_i). \tag{35}$$

The differentiation of $s_i(t)$ is

$$\dot{s}_i \approx -\sigma|s_i|^\mu \operatorname{sign}(s_i). \tag{36}$$

According to Proposition 1, it follows that the error system states will be attracted to the sliding surface and stabilized to zero within a finite time.

The dashed lines in Fig. 3 show the synchronization errors between the new chaotic system and the Lorenz system. It is clear that our proposed control strategy can stabilize the error system faster than the conventional control scheme. The simulation results confirm the theoretical results.

4.2. Example 2: Synchronize chaotic systems under disturbances

In order to show the robustness of the proposed control scheme, we turn to the new chaotic system and the Lorenz system under internal uncertainties and external disturbances.

The uncertain and perturbed new chaotic system is given by

$$\begin{cases} \dot{x}_1 = 0.5(-x_1) + x_2^2 + \Delta f_1(\boldsymbol{x}) + d_1^{\mathrm{m}}, \\ \dot{x}_2 = 2.5x_2 - x_1x_3 + \Delta f_2(\boldsymbol{x}) + d_2^{\mathrm{m}}, \\ \dot{x}_3 = x_2 - 4x_3 + \Delta f_3(\boldsymbol{x}) + d_3^{\mathrm{m}}; \end{cases} \tag{37}$$

and the uncertain and perturbed Lorenz chaotic system is

$$\begin{cases} \dot{y}_1 = 10(y_2 - y_1) + \Delta g_1(y) + d_1^{\mathrm{s}}, \\ \dot{y}_2 = 30y_1 - y_2 - y_1y_3 + \Delta g_2(y) + d_2^{\mathrm{s}}, \\ \dot{y}_3 = -\frac{8}{3}y_3 + y_1y_2 + \Delta g_3(y) + d_3^{\mathrm{s}}, \end{cases} \tag{38}$$

where $\Delta f_i(\boldsymbol{x})$ and $\Delta g_i(\boldsymbol{x})$ are the internal uncertainties, $\Delta f_1(\boldsymbol{x}) = 0.15\sin(t)x_1$, $\Delta f_2(\boldsymbol{x}) = 0.2\sin(t)x_2$, $\Delta f_3(\boldsymbol{x}) = 0.25\sin(t)x_3$, $\Delta g_1(\boldsymbol{y}) = 0.1\cos(t)y_1$, $\Delta g_2(\boldsymbol{y}) = 0.15\cos(t)y_2$, $\Delta g_3(\boldsymbol{y}) = 0.1\cos(t)y_3$; d_i^{m} and d_i^{s} are the external disturbances, $d_1^{\mathrm{m}}, d_2^{\mathrm{m}}$, and d_3^{m} are uniformly distributed random noises with an amplitude of 0.3 as illustrated in Fig. 4, $d_1^{\mathrm{s}}, d_2^{\mathrm{s}}$, and d_3^{s} are uniformly distributed random noises with an amplitude of 0.5 as shown in Fig. 5.

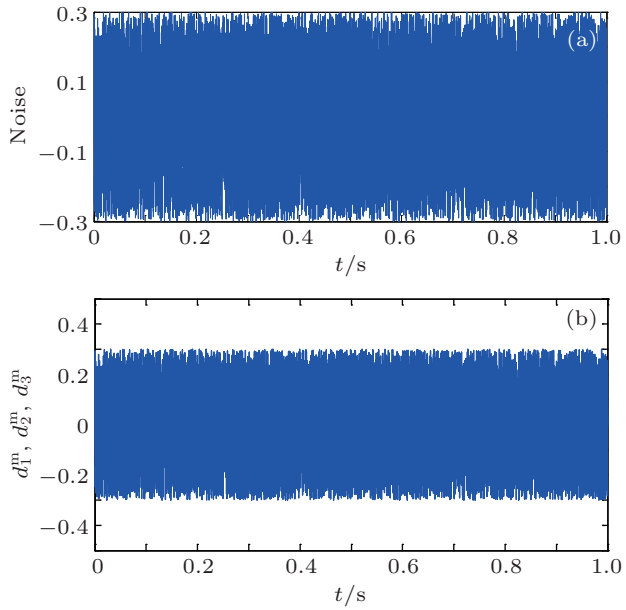


Fig. 4. (color online) Uniformly distributed random noises with an amplitude of 0.3.

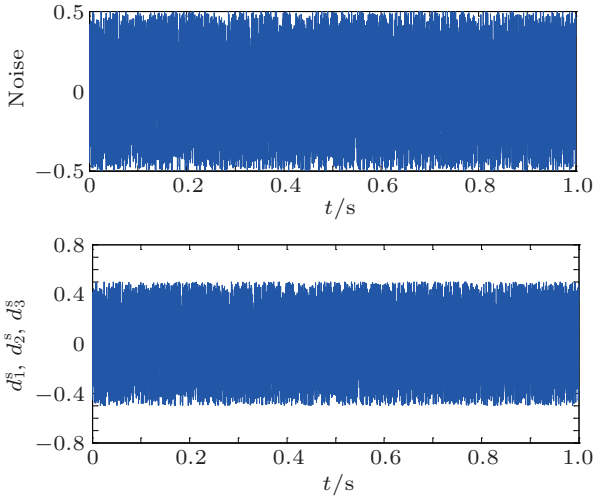


Fig. 5. (color online) Uniformly distributed random noises with an amplitude of 0.5.

By using Eq. (31) as the sliding surface, the control law can be obtained as

$$\begin{aligned} u_i = {} & A_i\boldsymbol{x} - B_i\boldsymbol{y} + f_i(\boldsymbol{x}) - g_i(\boldsymbol{y}) \\ & - (\alpha_i|x_i| + \beta_i|y_i| + D_i^{\mathrm{s}} + D_i^{\mathrm{m}})\frac{s_i}{|s_i| + \varepsilon} \\ & - 5\frac{e_i}{|e_i| + \varepsilon} - 10e_i - 5\frac{s_i}{|s_i| + \varepsilon} - 10s_i, \end{aligned} \tag{39}$$

where $\alpha_1 = 0.15$, $\alpha_2 = 0.2$, $\alpha_3 = 0.25$, $\beta_1 = 0.1$, $\beta_2 = 0.15$, $\beta_3 = 0.1$, $D_1^{\mathrm{s}} = D_2^{\mathrm{s}} = D_3^{\mathrm{s}} = 0.5$, and $D_1^{\mathrm{m}} = D_2^{\mathrm{m}} = D_3^{\mathrm{m}} = 0.3$.

The proposed finite-time sliding mode control scheme is used to synchronize the uncertain and disturbed new chaotic system and Lorenz chaotic system. The evolution of the synchronization errors are shown in Fig. 6. As can be seen from Fig. 6, our proposed finite-time sliding mode control scheme can suppress the disturbances and uncertainties effectively and achieve the synchronization rapidly, which shows the robustness of the proposed finite-time sliding mode controller against internal uncertainties and external disturbances.

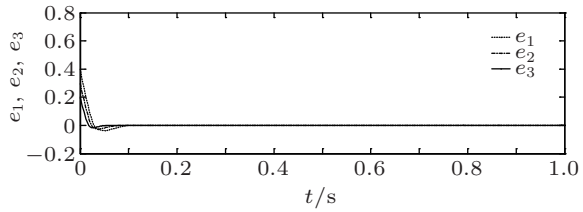


Fig. 6. Evolution of the synchronization errors between an uncertain and disturbed new chaotic system and Lorenz chaotic system.

4.3. Example 3: Application in secure communication

In order to show that our control scheme can decrypt the masked signal effectively, we consider three different generated signals with the same amplitude of one and the same frequency of 0.1, i.e. sine-wave $m_1(t)$, square wave $m_2(t)$ and triangular wave $m_3(t)$. These message signals are added to the second state of the master system to produce noise-like signals

shown in Figs. 8, 10, and 12, respectively. The resulting message is transmitted to the receiver through an additive white Gaussian noise communication channel with a signal-to-noise ratio (SNR) of 40 dB. At the receiving location, there is a controller to realize synchronization between the master system and the slave system. The second state of the slave system is subtracted from the resulting message and the message signal can be recovered as shown in Figs. 9, 11, and 13, respectively. The whole process is depicted in Fig. 7. The equations of the sender are

$$\begin{cases} \dot{x}_1 = 0.5(-x_1) + x_2^2 + \Delta f_1(\boldsymbol{x}) + (x_2 + m(t)), \\ \dot{x}_2 = 2.5x_2 - x_1x_3 + \Delta f_2(\boldsymbol{x}), \\ \dot{x}_3 = x_2 - 4x_3 + \Delta f_3(\boldsymbol{x}); \end{cases} \tag{40}$$

and those of the receiver are

$$\begin{cases} \dot{y}_1 = 10(y_2 - y_1) + \Delta g_1(\boldsymbol{y}) + (x_2 + m(t) + n(t)) + u_1, \\ \dot{y}_2 = 30y_1 - y_2 - y_1y_3 + \Delta g_2(\boldsymbol{y}) + u_2, \\ \dot{y}_3 = -\frac{8}{3}y_3 + y_1y_2 + \Delta g_3(\boldsymbol{y}) + u_3, \end{cases} \tag{41}$$

where $m(t)$ denotes the message signal and $n(t)$ represents the white Gaussian noise.

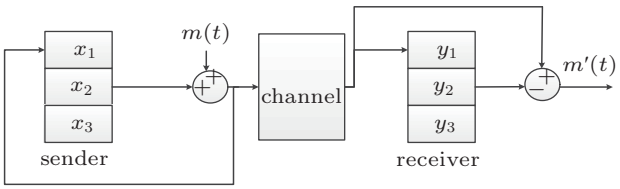


Fig. 7. Block diagram of secure communication.

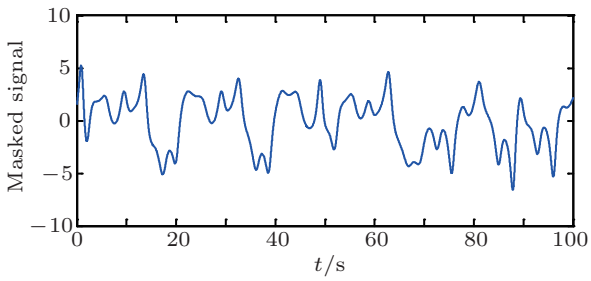


Fig. 8. (color online) Time evolution of masked sine-wave signal.

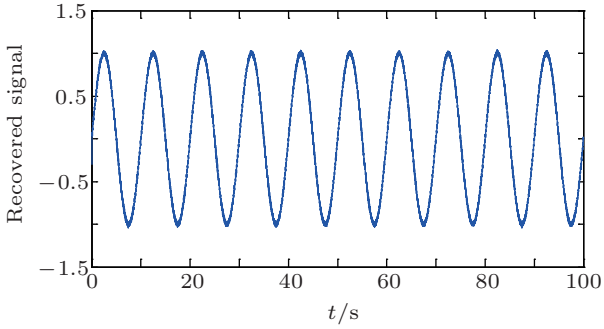


Fig. 9. (color online) Recovered sine-wave signal.

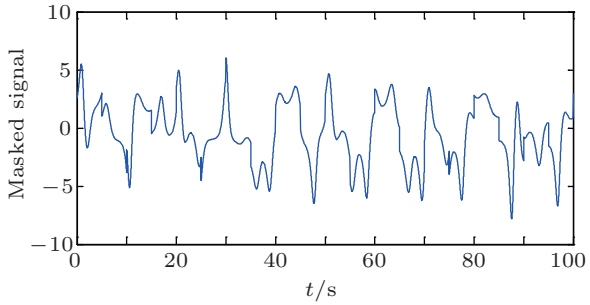


Fig. 10. (color online) Time evolution of masked square-wave signal.

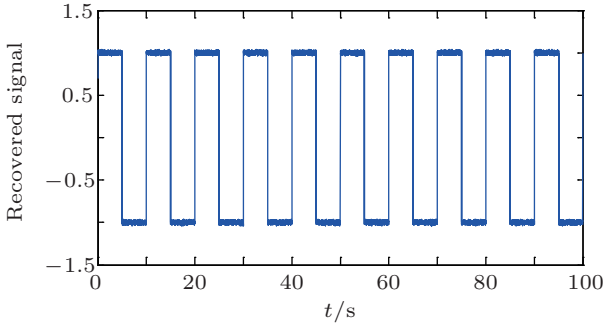


Fig. 11. (color online) Recovered square-wave signal.

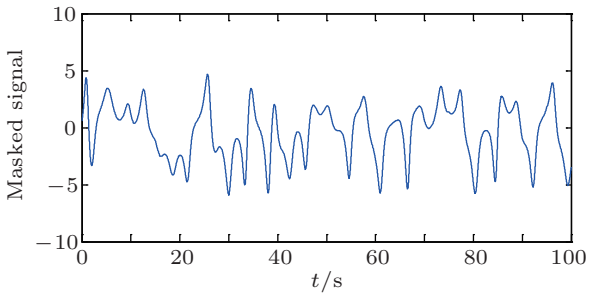


Fig. 12. (color online) Time evolution of masked triangular-wave signal.

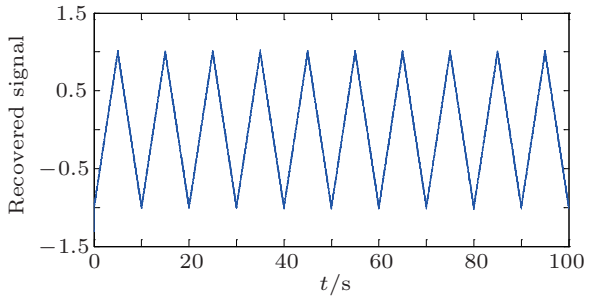


Fig. 13. (color online) Recovered triangular-wave signal.

As can be seen from Figs. 9, 11, and 13, although the recovered signals are slightly distorted due to the white Gaussian noise interference, the information can still be decoded from the recovered signals correctly. To compare the communication performances of the proposed control scheme and the conventional control scheme in the context of channel noise, we compute the bit error rates (BERs) for different SNRs. Figure 14 shows the results. It can be observed that the BER decreases monotonically with the increase of the SNR and the

BER reaches zero at an SNR of about 10 dB for the proposed control scheme. In comparison with the conventional finite-time sliding mode control scheme, our scheme shows a good BER performance. It follows that our control scheme achieves satisfactory outcomes when applied to the secure communication.

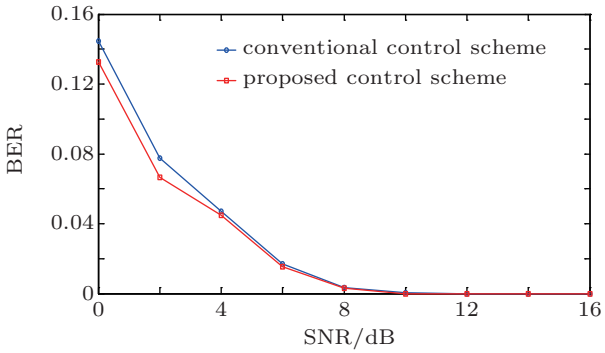


Fig. 14. (color online) BER versus SNR for the two schemes.

5. Conclusion

Optimizing the synchronization time is a challenging task for the real applications of control theory. In this paper, we propose a finite-time sliding mode control to realize the synchronization between two different chaotic systems. We prove that our control scheme has a faster convergence rate than conventional finite-time sliding mode control which has the form $\dot{s} = -k|s|^{\alpha}\,\mathrm{sign}(s)$. In order to show the effectiveness of our control scheme, we first show that our control scheme takes less time to synchronize a new chaotic system evolved from the Liu system and a Lorenz chaotic system than the conventional finite-time sliding mode control. Next, we synchronize the new chaotic system and the Lorenz chaotic system with internal uncertainties as well as external disturbances and show that our control scheme has strong robustness against internal uncertainties and external disturbances. Finally, we apply our control scheme to secure communications and achieve satisfactory results.

References

[1] Wang X Y, Zhang N, Ren X L and Zhang Y L 2011 *Chin. Phys. B* **20** 020507

[2] Tang Y, Fang J A and Miao Q Y 2009 *Neurocomputing* **72** 1694

[3] Blasius B, Huppert A and Stone L 1999 *Nature* **399** 354

[4] Schäfer C, Rosenblum M G, Abel H H and Kurths J 1999 *Phys. Rev. E* **60** 857

[5] Argyris A, Syvridis D, Larger L, Annovazzi L V, Colet P, Fischer I, García O J, Mirasso C R, Pesquera L and Shore K A 2005 *Nature* **438** 343

[6] Fischer I, Liu Y and Davis P 2000 *Phys. Rev. A* **62** 011801

[7] Iu H H C and Tse C K 2000 *IEEE Trans. Circuits Syst. I: Fundam. Theory Appl.* **47** 913

[8] Wang X Y and Zhang H 2013 *Chin. Phys. B* **22** 048902

[9] Xie Q X and Chen G R 2002 *Math. Comput. Model.* **35** 145

[10] Chen G R and Dong X N 1998 *From Chaos to Order: Methodologies, Perspectives and Applications* (Singapore: World Scientific) pp. 537–617, ISBN: 9810225695 9789810225698

[11] Pecora L M and Carroll T L 1990 *Phys. Rev. Lett.* **64** 821

[12] Agiza H N and Yassen M T 2001 *Phys. Lett. A* **278** 191

[13] Chai Y, Lu L and Chen L Q 2012 *Chin. Phys. B* **21** 030506

[14] Liu J G 2013 *Chin. Phys. B* **22** 060510

[15] Wang Y J, Hao J N and Zuo Z Q 2010 *Phys. Lett. A* **374** 2024

[16] Salarieh H and Alasty A 2009 *Commun. Nonlinear Sci. Numer. Simul.* **14** 508

[17] Kwon O M, Park M J, Park J H, Lee S M and Cha E J 2013 *Chin. Phys. B* **22** 110504

[18] Wang D F, Zhang J Y and Wang X Y 2013 *Chin. Phys. B* **22** 100504

[19] Kuntanapreeda S 2009 *Phys. Lett. A* **373** 2837

[20] Wang X Y and Song J M 2009 *Commun. Nonlinear Sci. Numer. Simul.* **14** 3351

[21] Yau H T and Shieh C S 2008 *Nonlinear Anal. Real World Appl.* **9** 1800

[22] Liu L, Liang D L and Liu C X 2012 *Nonlinear Dyn.* **69** 1929

[23] Zhu D R, Liu C X and Yan B N 2012 *Chin. Phys. B* **21** 090509

[24] Chuang C F, Sun Y J and Wang W J 2012 *Chaos* **22** 043108

[25] Cai N, Li W Q and Jing Y W 2011 *Nonlinear Dyn.* **64** 385

[26] Liu P 2013 *Chin. Phys. B* **22** 070501

[27] Gholizadeh H, Hassannia A and Azarfar A 2013 *Chin. Phys. B* **22** 010503

[28] Aghababa M P and Feizi H 2012 *Trans. Inst. Meas. Control* **34** 990

[29] Vincent U E and Guo R 2011 *Phys. Lett. A* **375** 2322

[30] Wang H, Zhang X L, Wang X H and Zhu X J 2012 *Nonlinear Dyn.* **69** 1941

[31] Wang D F, Zhang J Y and Wang X Y 2013 *Chin. Phys. B* **22** 040507

[32] Wang H, Han Z Z, Xie Q Y and Zhang W 2009 *Commun. Nonlinear Sci. Numer. Simul.* **14** 2728

[33] Yang L and Yang J Y 2011 *Commun. Nonlinear Sci. Numer. Simul.* **16** 2405

[34] Liu Y F, Yang X G, Miao D and Yuan R P 2007 *Acta Phys. Sin.* **56** 6250 (in Chinese)

[35] Aghababa M P, Khanmohammadi S and Alizadeh G 2011 *Appl. Math. Model.* **35** 3080

[36] Li S H and Tian Y P 2003 *Chaos, Solitons and Fractals* **15** 303

[37] Aghababa M P and Feizi H 2012 *Chin. Phys. B* **21** 060506

[38] Zhao Z S, Zhang J and Sun L K 2013 *ISRN Appl. Math.* **2013** 320180

[39] Slotine J and Li W 1991 *Applied Nonlinear Control* (New Jersey: Prentice Hall), ISBN: 0-13-040890-5

[40] Liu C X 2011 *Theory and Application of Fractional Order Chaotic Circuit* (Xi'an: Xi'an Jiaotong University Press) p. 21 (in Chinese), ISBN: 9787560525921

[41] Liu C X, Liu T, Liu L and Liu K 2004 *Chaos, Solitons and Fractals* **22** 1031

[42] Lorenz E N 1963 *J. Atmos. Sci.* **20** 130